Submitted to: International Workshop on Hydrogen in Materials & Vacuum Systems
JLAB, Newport News, VA, November 11-13, 2002

BNL-71032-2003-CP

Hydrogen and Its Desorption in RHIC[11]

H.C. Hseuh

Collider-Accelerator Department
Brookhaven National Laboratory
Upton, NY 11973, USA

Abstract. Hydrogen is the dominating gas specie in room temperature, ultrahigh vacuum systems of particle accelerators and storage rings, such as the Relativistic Heavy Ion Collider (RHIC) at Brookhaven. Rapid pressure increase of a few decades in hydrogen and other residual gases was observed during RHIC's recent high intensity gold and proton runs. The type and magnitude of the pressure increase were analyzed and compared with vacuum conditioning, beam intensity, number of bunches and bunch spacing. Most of these pressure increases were found to be consistent with those induced by beam loss and/or electron stimulated desorption from electron multi-pacting.

INTRODUCTION

RHIC accelerates, stores and collides highly relativistic particle beams from proton to gold with energies up to 250 GeV/nucleon for nuclear physics research. RHIC has a circumference of 3.8 km and comprises two interweaving rings (named yellow ring and blue ring) that intersect with each other at six locations as shown schematically in Fig. 1. There are three distinct vacuum systems in RHIC proper. The insulating vacuum vessels house the helium-cooled super-conducting magnets. The cold beam tubes (cold bore) pass through the center of the super-conducting magnets. The room temperature (warm bore) beam vacuum regions house the injection, acceleration, instrumentation and experimental regions.

The total length of cold bore and cryostats is ~ 6.4 km, divided into 12 arc sections and 24 triplet sections. Each 494m arc section consists of a continuous (without vacuum barriers) cryostat, housing 64 super-conducting magnets interconnected to form a continuous cold beam tube. The two adjacent triplet magnet strings reside within a common cryostat due to their proximity. The total length of warm bore is approximately 1.2 km, consisting of the 24 Q3-Q4 insertion regions, the 12 DX-D0 final focusing regions and the six interaction regions (called IP). The warm bore makes up roughly 16% of the RHIC circumference. The warm sections are pumped by ion pumps and titanium sublimation pumps, and monitored with cold cathode gauges (CCG) every 10 m. Most of the warm sections are in-situ bakeable to 250°C. The layout of the vacuum equipment for one-twelfth of the collider is shown in Fig. 1.

[1] Work performed under the auspices of the U.S. Department of Energy

RHIC Beam Vacuum Requirements

The warm bore design vacuum is $<5\times10^{-10}$ Torr ($\sim1.7\times10^{+7}$ molecules/cm^3) consisting of mostly hydrogen (H_2). The cold bore design vacuum is $<1\times10^{-11}$ Torr ($\sim2\times10^{+7}$ molecules/cm^3 after correcting for thermal transpiration) consisting of only H_2 and He since all other gases will condense on the 4K surfaces. Elastic and inelastic scattering from beam-residual gas interactions were considered when determining the vacuum requirements for the worst case, i.e. Au at injection energy of ~10 GeV/u. The elastic scattering causes the growth of the transverse emittance. Using the Fokker-Planck diffusion equation, the growth rate at the design vacuum level is $\sim10^{-4}$ mm.mrad/hr [1] which is insignificant in comparison with the emittance growth due to intra-beam scattering. The inelastic scattering includes electron capture and nuclear scattering, which cause immediate beam loss. The total electron capture cross section is $\sim10^{-25}$ cm^2 for Au at 10 GeV/u [2]. The nuclear scattering cross section is proportional to the geometrical cross section and is $\sim10^{-24}$ cm^2 for Au. The beam-gas lifetime dominated by the nuclear scattering will be several hundred hours for Au [3] at the design vacuum of $2\times10^{+7}$ molecules/cm^3, much longer than the ten-hour intra-beam scattering lifetime. Background noise to the experiment detector, due to beam-residual gas nuclear scattering at and near experimental regions puts the most stringent requirement on RHIC beam vacuum systems. At the design vacuum level, the probability of beam-gas interaction ±40m around the collision point will be $\sim1\times10^{-4}$ interactions per bunch per crossing. The total beam-gas rate will be $\sim10^3$ Hz which is comparable to the beam-beam rate [4] at the design luminosity of 10^{-26}cm^{-2} s^{-1}.

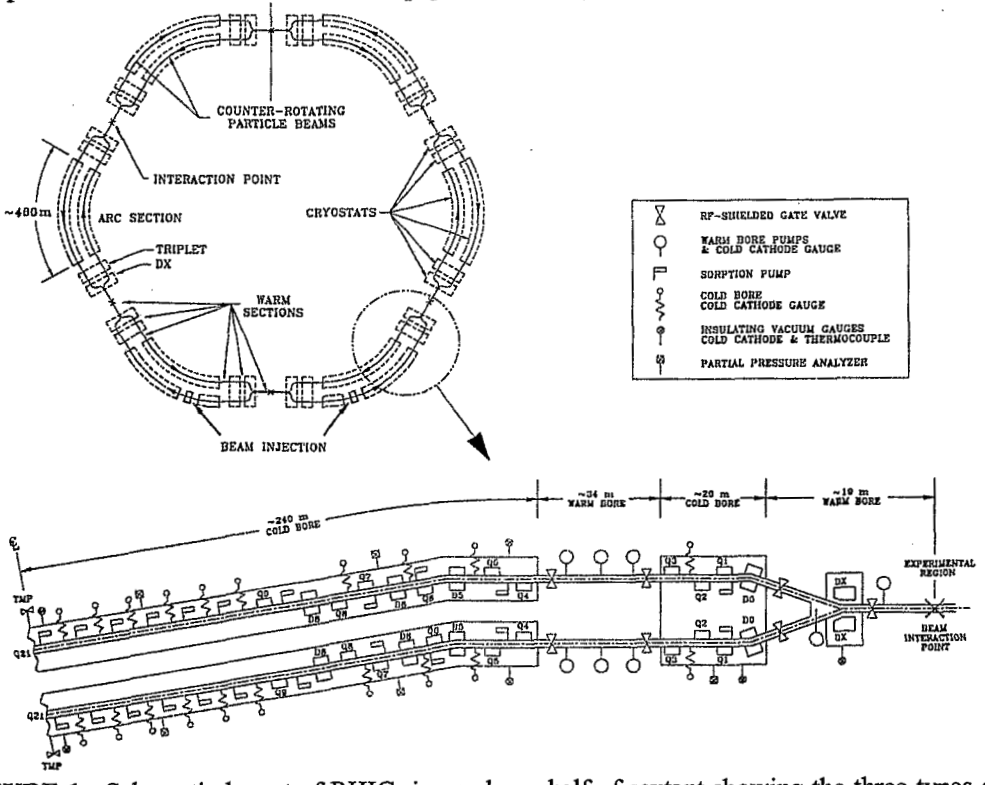

FIGURE 1. Schematic layout of RHIC ring and one-half of sextant showing the three types of warm vacuum regions, the Q3-Q4 insertion, the final DX focusing and the interaction region.

Performance of RHIC Beam Vacuum Systems

The construction and commissioning of RHIC was completed in 1999. The collider had reached 65% of the design energies and 10% of the design luminosity during the 1st physics run in 2000, and achieved the full design energy and 50% of the design luminosity during the 2001 physics run.

The vacuum systems have performed well and met the requirements for collider operations over the last few years. The average pressures of the warm sections have reached below the design vacuum level, owing to the gradual bakeouts of some warm sections around the experimental regions over the last three years. After in-situ bakes, vacuum levels are usually at $< 1x10^{-10}$ Torr with majority residual gas being hydrogen, thereby decreasing the background noise to the detectors.

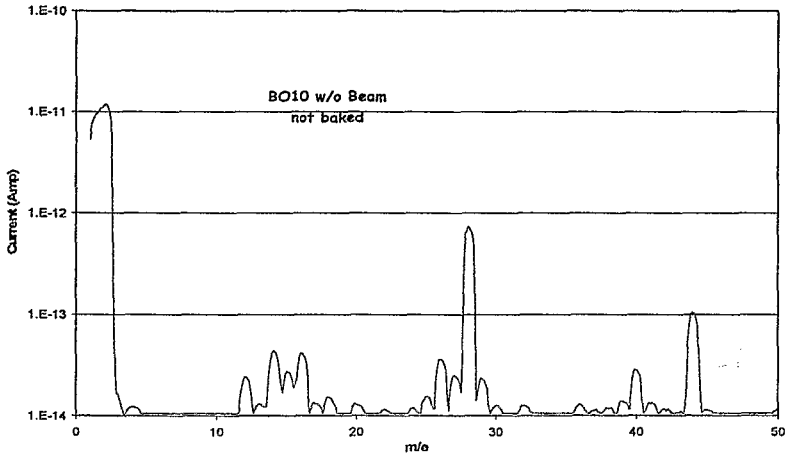

FIGURE 2. Typical RGA scan of a not baked warm section with major gas being hydrogen.

Prior to the magnet cool down, the cold bore is pumped down to $< 10^{-4}$ Torr with a turbomolecular pump. After cool down to 4.5K, the CCGs read mid-10^{-10} Torr range when the true pressure in the cold bore is $< 10^{-11}$Torr. The high readings are due to the localized outgassing of the room temperature gauge conduits. The usefulness of the CCGs in monitoring the cold bore He pressure was studied during RHIC first sextant test [5] and found to be capable of detecting He pressure changes down to ~10^{-11} Torr.

PRESSURE RISES IN RHIC

No notable changes in pressure were observed during the 1999 beam commissioning and the 2000 Collider operation. However, pressure rises of several decades were measured in the warm bore sections during 2001 high-intensity gold (Au) and proton runs. These rapid pressure rises sometimes exceeded the CCG set points (usually at $5x10^{-7}$ Torr) for gate valve interlocks and aborted the beams. The pressure rises were especially prominent during 110-bunch Au injection and became one of the major intensity-limiting factors for RHIC operation. Using logged CCG and residual gas analyzer (RGA) data, and the beam current monitor readings, the pressure

rises in a few ramps and stores were analyzed and discussed within the frame work of ion desorption, electron multi-pacting and direct beam loss.

Pressure Increase during Gold Runs

Several types of pressure rises were observed during the 2001 Au runs. Typical cases of pressure rises during stable ramps and stores for 55-bunch mode (with ~ 200 nsec bunch spacing) are shown in Fig. 3 where the initial bunch intensity was ~ $6x10^8$ Au^{+79} (total of > $3x10^{10}$ Au ions). The pressure of some unbaked sections (e.g. BI9 and YI10) would increase by a decade or less, consisting mostly of H_2, H_2O and CO. The pressure would then gradually decrease as the stored beam current fell. There were no notable pressure rises in most baked sections, e.g. IP10.

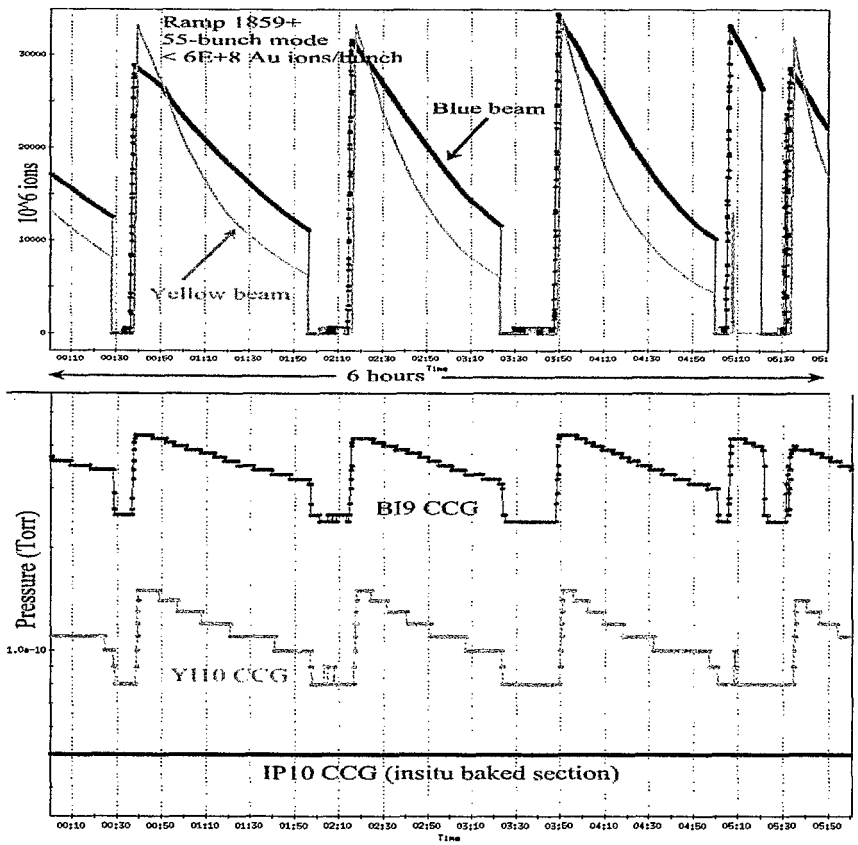

FIGURE 3. RHIC pressure rises during stable gold stores with initial bunch intensity of ~ $6x10^8$ Au ions x 55 bunches. The pressure increase is usually less than one decade in not-baked sections.

However, once the bunch intensity was raised beyond $8x10^8$ ions or when RHIC operated in 110-bunch mode (with ~ 100 nsec bunch spacing), rapid pressure rises of a few decades were observed during injection and ramp, particularly at several specific warm sections. Typical cases are shown in Fig. 4 for both 55- and 110-bunch modes. With 110-bunch mode (left side of figure), the pressure started to increase at $1x10^{10}$ ions for BO11 (that is blue ring outer 11 o'clock insertion region). The pressure exceeded the CCG set points after only 39 bunches (for a total of ~ $3x10^{10}$ Au ions) were injected, which caused the beam abort by a vacuum interlock. the other important

observation is that the pressure would peak at constant intensity, and then reached another plateau with further injection.

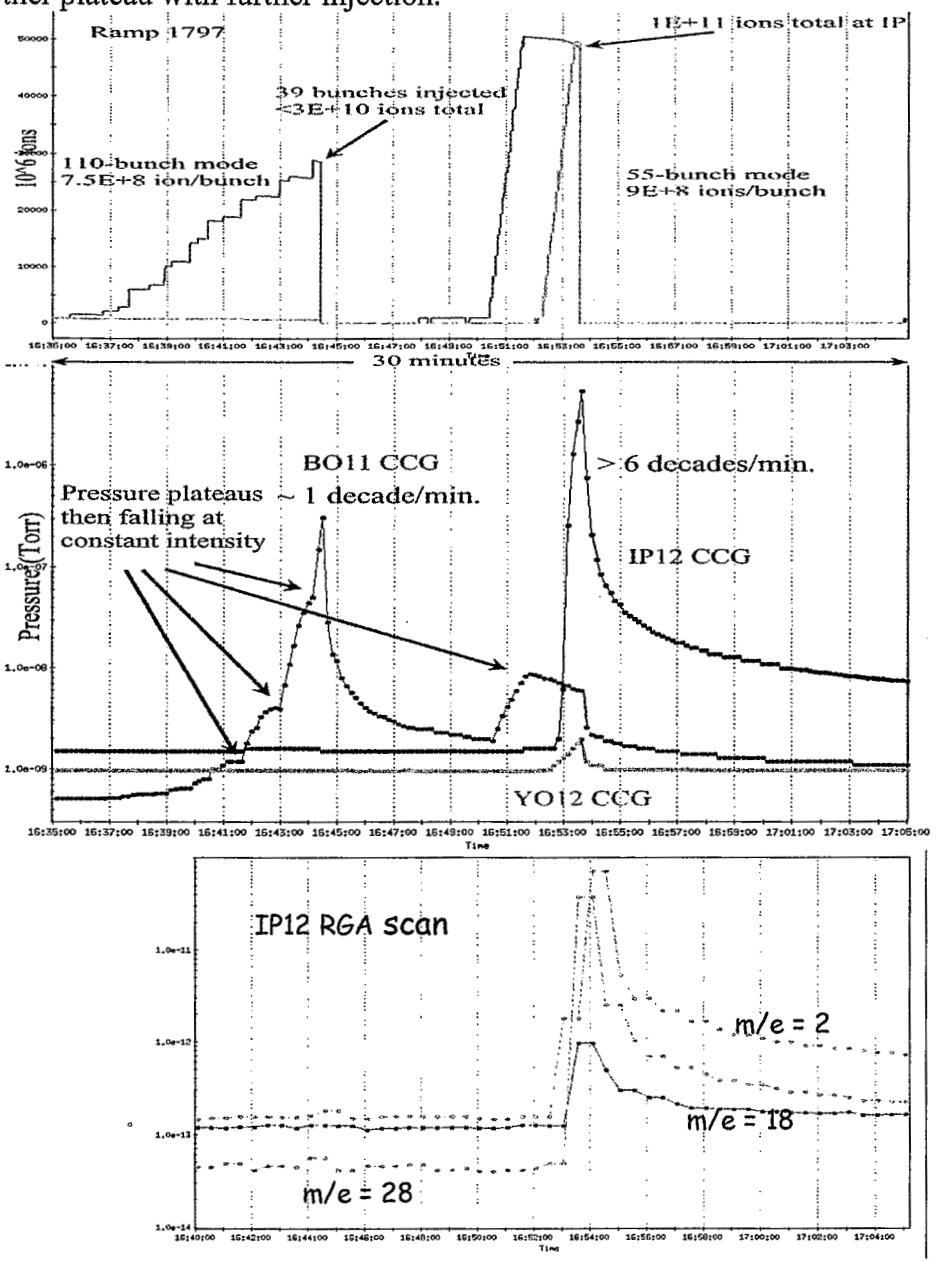

FIGURE 4. Pressure rises during 110-bunch and 55-bunch Au injections. The magnitude of pressure rise at 110-bunch mode is much higher than that of 55-bunch mode even though the total intensity is lower.

The pressure rise in BO11 with the 110-bunch mode was much higher than that of 55-bunch mode (right side) even though the total intensity was much lower. At 55-bunch mode, the pressure at IP12 remained unchanged till the total current (sum of both B & Y) reached a threshold of ~ 7×10^{10} Au ions, then rose sharply and caused a vacuum interlock at a total intensity of 1×10^{11} ions. The relative increase of CO at IP12 is higher than H_2 indicating that surface desorption over bulk desorption.

Pressure Increase during Proton Runs

Pressure rises during proton runs were in general much less than that during Au runs, even with similar total charges. This is due to the smaller ionization cross section of residual gas molecules ($\propto Z^2$) by proton than that by Au. Pressure instability was observed if the proton bunch intensity was raised beyond $8x10^{10}$ or when the machine was operated at 110-bunch mode, as shown in Fig. 5. In 110-bunch mode, the peak pressure of the YO12 was one decade lower than that of BO11 even with similar intensities. At BO11, the peak pressure for 55-bunch mode was much less than that of 110-bunch mode. Similar to the Au run, the intensity threshold for pressure rise at IP12 (with both beams) was ~ $7x10^{12}$ protons (55 bunches), much higher than those of BO11 and YO12 (with single beam). The pressure fell rapidly with the acceleration. None of the pressure rises during proton runs exceeded the vacuum interlock limits.

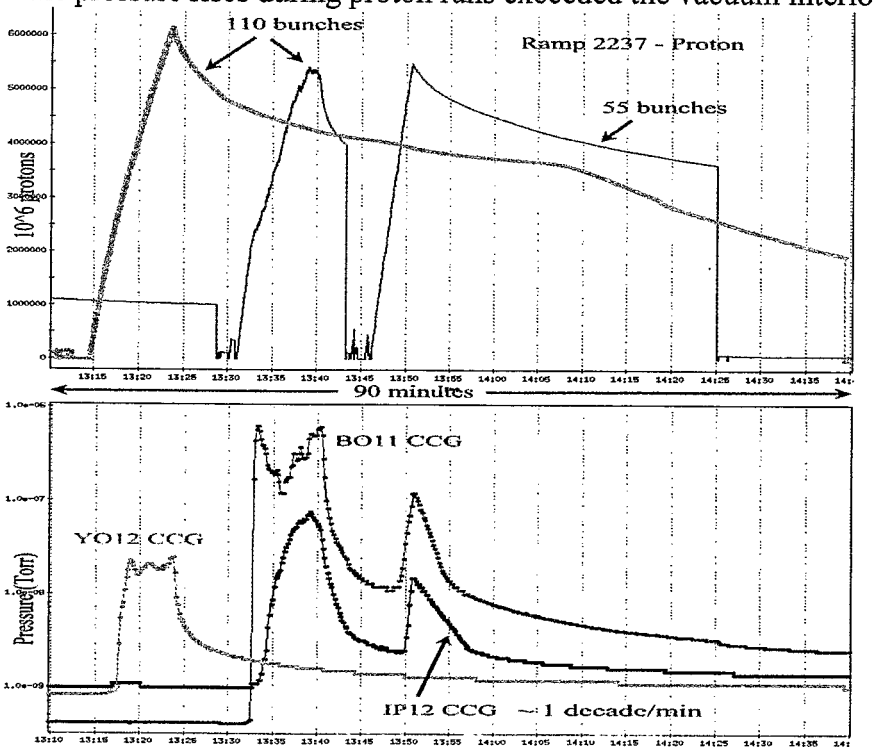

FIGURE 5. Pressure rises during proton runs, which are higher for 110-bunch mode than for 55-bunch modes even at similar intensity illustrating again the dependence on bunch spacing. The amount of increase is less than that of Au runs even the total charges are higher, mostly due to smaller ionization cross section by protons.

ANALYSIS OF PRESSURE RISES

Electron Multi-pacting and Saturation

There are several potential mechanisms causing the pressure rises. The electrons, from beam-residual gas ionization and other sources, heated up by the passing bunches, could bombard the vacuum wall and desorb more electrons (electron multi-

pacting or EMP) and molecules (electron stimulated desorption or ESD). EMP could be very sensitive to bunch spacing and bunch intensity, but less to total intensity, and usually reaches saturation at constant intensity [6] as shown in Fig. 6. In this 110-bunch Au run, the bunch intensity was relatively low. There was little increase in pressure in both B and Y, even though the total intensity was one of the highest reached. This suggests the absence of ion desorption, which would be proportional to total intensity. The rate of pressure rises was usually only a few decades per minute another indication of EMP instead of ion desorption and/or direct beam loss. Again, most desorbed gases were H_2 and CO with higher relative increase in CO than H_2 indicating surface desorption over bulk desorption.

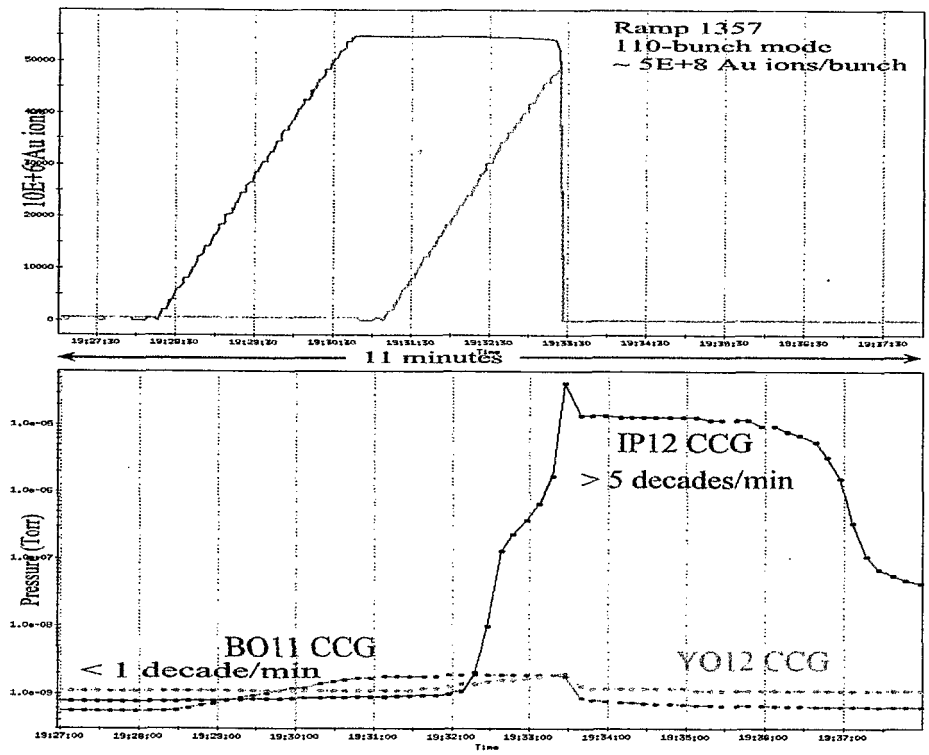

FIGURE 6. Little pressure rise with bunch intensity of $5x10^8$ Au ions at 110-bunch mode at single beam insertion regions during Au runs (total of $5.5x10^{10}$ ions), suggesting the dependence of pressure rise on bunch intensity instead of on total intensity.

Beam Loss Related Pressure Rise

Grazing-angle beam loss on the wall can desorb large amount of gas molecules [7]. Subsequent ionization by the circulating beam and the resulting electron and ion desorption can generate more gas molecules. A typical case is shown in Fig. 7. No significant pressure rises were observed at these sections until the start of acceleration, when beam loss occurred with a corresponding pressure increase at IP12. The beam loss increased rapidly over the next few seconds with a rapid pressure rise of over 10 decades per minute at IP12 before beam was aborted by the vacuum interlock. Assuming all of the beams were lost at IP12, with a known vacuum volume and no effective pumping at 10^{-5} Torr, ~ 10^7 molecules were generated per lost ion. This desorption yield by direct beam loss was much higher than those reported for heavy

ions of lower energies [7]. Contribution from electron and ion desorption could reduce this number somewhat. The relative partial pressure rises of CO and H_2 are similar in this case. This suggests that the stopping range of energetic heavy ions at grazing angle is much longer than that of the normal incidence electrons, causing more bulk H_2 desorption in addition to the surface desorption of CO. This is in contrast to the predominant surface desorption by EMP/ESD process.

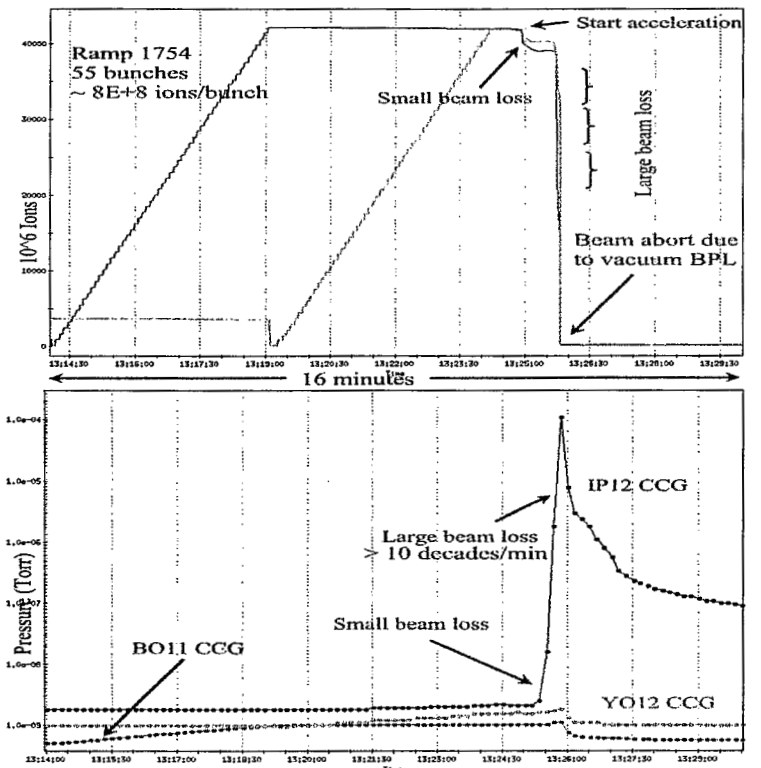

FIGURE 7. Direct beam loss induced pressure rises during Au acceleration.

Intensity Thresholds for Pressure Rises

The beam intensity thresholds at initial pressure rises for Au and proton can be estimated from a few high-intensity ramps. A typical case is shown in Fig. 8 for proton runs with 55 bunches. The thresholds for the start of pressure rises of various modes are summarized in Table I.

TABLE 1. Comparison of intensity thresholds for pressure rises among protons and Au, 55-bunch and 110-bunch, single-beam and two-beam.

	IP (two beams)	Insertion (one beam)
P – 55 bunches	$7x10^{12}$	$4x10^{12}$
P – 110 b	$6x10^{12}$	$2x10^{12}$
Au^{+79} ions – 55 b	$7x10^{10}$	$2x10^{10}$
Au^{+79} ions – 110 b	~ $6x10^{10}$	$1x10^{10}$
Au / P charge ratio	~ 0.8	~ 0.4

The thresholds for insertion regions are ~ $4x10^{+12}$ protons, while that of IP regions are ~ $7x10^{+12}$, almost twice as high. Little difference in thresholds was observed

between the 55- and 110-bunch modes, even though the final pressure rises are much higher for 110-bunch mode. The ratios of the total-charge thresholds between gold and proton beams depend on the bunch intensity therefore are approximate. The pressurize rises tend to reach saturation at the end of injection, start to decrease slowly before capture, and then fall rapidly when acceleration begins. This could be due to the reduced beam size and the resulted beam loss after capture and acceleration, which would not desorb enough residual gas molecules for further ionization to sustain the electron multi-pacting.

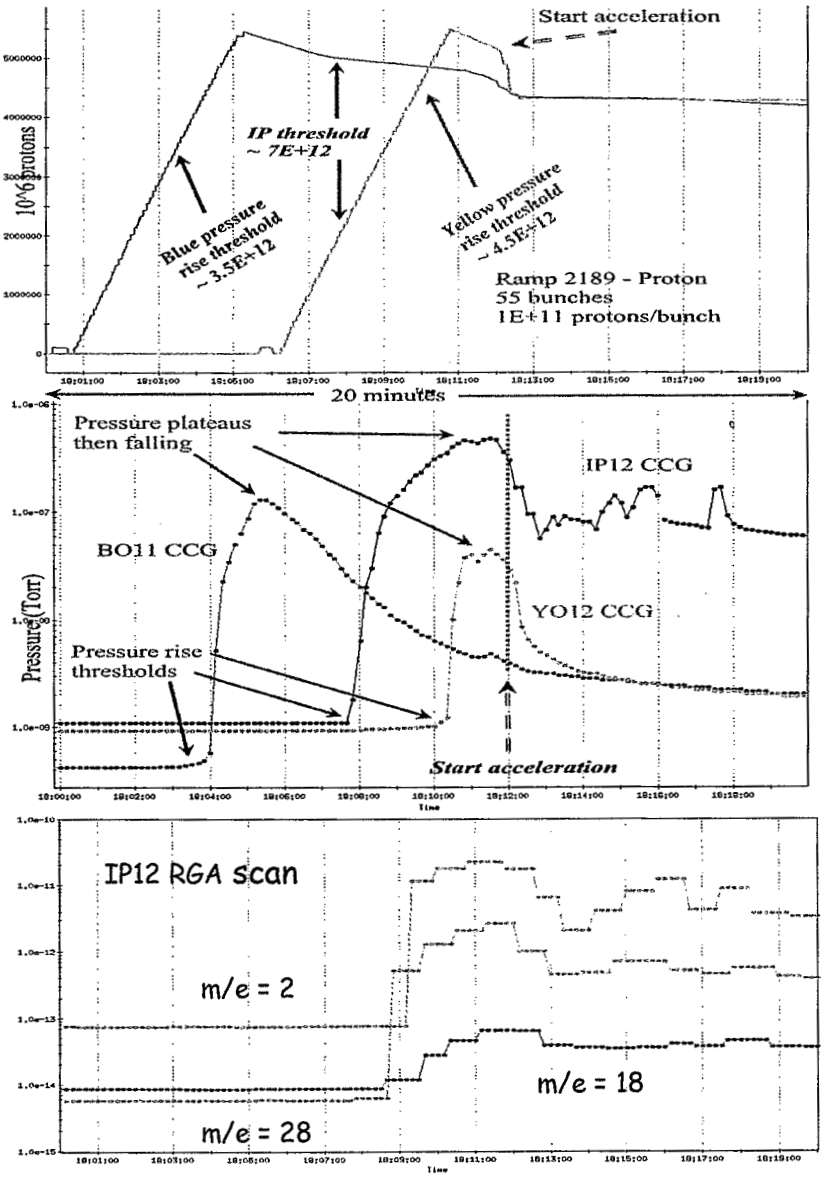

FIGURE 8. Intensity thresholds for pressure rises during proton injection. The pressure rises reach saturation at end of injection and RF capture then decrease rapidly after acceleration. The thresholds for two-beam (IP) regions are much higher than that of the single-beam (insertion) regions. Again, the main desorbed gas species are H_2 and CO, with the relative increase of CO larger or equal to that of H_2 indicating more surface desorption caused by EMP/ESD process.

SUMMARY

A few recent RHIC ramps were selected to illustrate two different types of pressure rises; one with slow pressure rises of a few decades per minute and usually reaching saturation at constant intensity, and the other with rapid increases of over ten decades per minute resulting in pressure run-away. The first type is more sensitive to bunch intensity and bunch spacing, and less dependent on the total intensity. This type of pressure rise is consistent with that of electron multi-pacting and electron stimulated desorption, instead of ion induced desorption which is more dependent on the total intensity. The relative pressure rise for CO is equal or higher than that of H_2 indicating predominant surface desorption. The second type of desorption is thought to be due to direct beam loss at glancing angle and subsequent desorption [7]. The relative pressure rise for CO is similar to that of H_2 indicating both bulk and surface desorption, and probably caused by the deep penetration of the energetic heavy ions into the bulk of chamber wall.

Electron detectors and solenoids are being installed in a few offending warm sections during the present shut down to measure the electron density and to confine the electrons along the beam axis for the next high intensity run. These measurements will be compared with those of ion desorption, EMP/ESD and direct beam loss [6]. Additional warm sections have also been baked to reduce the total pressure, the molecular desorption yields and the secondary electron yields, thus mitigating the ESD process.

ACKNOWLEDGMENTS

The author will like to thank Loralie Smart of Collider-Accelerator (C-A) Vacuum Group for her assistance in collecting vacuum data and Shou-Yuan Zhang of C-A Accelerator Physics for illuminating the potential of electron multi-pacting and desorption in RHIC vacuum pipes under various beam parameters.

REFERENCES

1. M. J. Rhoades-Brown and M. A. Harrison, RHIC Technical Note #106, BNL-47070, Dec. 1991.
2. R. Anholt and U. Becker, Phys. Rev. A36, 4628 (1987).
3. D. Trbojevic, RHIC/AP Report #136. Oct., 1997.
4. S. White, Private Comm., Oct. 1991.
5. H.C. Hseuh and E. Wallen, J. Vac. Sci. Technol., A16, 1145 (1998).
6. S.Y. Zhang, BNL C-A/AP/67, Jan., 2002; H.C. Hseuh, et al., Proc. EPAC02, (2002) (in press).
7. J. Hansen, et al. LHC/VAC 2001-007, July 2001 ; E. Mahner, et al. Phys. Rev. Special Topics – Accelerators and Beams, (in press).